Obrabotka metallov (tekhnologiya, oborudovanie, instrumenty) = Metal Working and Material Science. 2025 vol. 27 no. 3 pp. 122–136
ISSN: 1994-6309 (print) / 2541-819X (online)
DOI: 10.17212/1994-6309-2025-27.3-122-136

NSTU NETI

Obrabotka metallov - Metal Working and Material Science

Journal homepage: http://journals.nstu.ru/obrabotka_metallov

Investigation of the process of surface decarburization of steel 20 after cementation and heat treatment

Yulia Karlina [1, a, *], ***Vladimir Konyukhov*** [2, 3, b], ***Tatiana Oparina*** [2, c]

[1] National Research Moscow State University of Civil Engineering, 26 Yaroslavskoe Shosse, Moscow, 129337, Russian Federation
[2] Irkutsk National Research Technical University, 83 Lermontova str., Irkutsk, 664074, Russian Federation
[3] Cherepovets State University, 5 Lunacharsky pr., Cherepovets, 162600, Russian Federation

[a] https://orcid.org/0000-0001-6519-561X, jul.karlina@gmail.com; [b] https://orcid.org/0000-0001-9137-9404, konyukhov_vyu@mail.ru;
[c] https://orcid.org/0000-0002-9062-6554, martusina2@yandex.ru

ARTICLE INFO

Article history:
Received: 28 February 2025
Revised: 13 March 2025
Accepted: 14 May 2025
Available online: 15 September 2025

Keywords:
Carbon
Ferrite
Martensite
Heating
Cementation
Tempering
Temperature
Cooling
Equalizing,
Duration
Decarbonization
Hardness

ABSTRACT

Introduction. In industry, the method of carburizing with a solid carburizer is used to saturate the surface layer with carbon. In practice, it is necessary to prevent or reduce surface decarburization of steel as much as possible, either by using a protective atmosphere or by heating under conditions in which the oxidation process of the metal surface layer occurs faster than the decarburization process. During decarburization, a ferrite structure is formed in the surface layer, which, under contact loads, reduces the resistance to crack initiation and increases the probability of fatigue failure of the product as a whole. **The purpose of this work** is to evaluate the effect of heating temperature during carburizing and subsequent hardening, as well as equalizing period, on the depth of the decarburized layer during chemical-thermal treatment of low-carbon steel. **Research methods.** The chemical composition of the steel as delivered was determined. The analyses were performed using an optical emission spectrometer, model *LAVFA18B Spectrolab*. For the study, unalloyed hypoeutectoid Steel 20 was selected, with an initial ferrite-pearlite microstructure. The samples had a rectangular shape with average dimensions of 50 mm × 10 mm × 10 mm. Carbon saturation was carried out on one side (from the side of the poured carburizer, while the reverse surface of the samples was protected by a layer of clay). The samples were placed in a metal container, filled with carburizer in a 25–30 mm layer, closed with a lid, and sealed. Carbon saturation was carried out at 900 °C for 4–8 hours. After that, the box with samples was taken out of the furnace and cooled in air. Quenching was carried out in a furnace in air (humidity was not measured) at furnace heating temperatures of T = 780 °C, 850 °C, and 950 °C with a equalizing period of 4.6 h in a laboratory electric resistance furnace with a chamber volume of V = 22 dm³. Metallographic examination and microhardness measurements were performed. **Results and discussion.** During the experiments, it was noted that the heating temperature for carburizing and quenching plays an important role in decarburization. At a temperature of 700 °C, the decarburization phenomenon was not observed, indicating that the decarburization reaction did not occur below this temperature. When the temperature exceeds 750 °C, the samples exhibit obvious decarburization, and the ferrite structure is columnar, oriented perpendicular to the decarburized surface. A partial decarburized layer appears in the samples at 850 °C, and the thickness of the full decarburized layer decreases. Above 900 °C, the sample mainly shows a partial decarburized layer because, at this temperature, the steel structure is fully austenitic. Above 1,000 °C, the layer thickness increases rapidly, showing exponential growth. The experiments also demonstrated the effect of heating and equalizing periods on the depth of the decarburized layer. The presented results will be useful in chemical-thermal treatment of products requiring high surface hardness.

For citation: Karlina Yu.I., Konyukhov V.Yu., Oparina T.A. Investigation of the process of surface decarburization of steel 20 after cementation and heat treatment. *Obrabotka metallov (tekhnologiya, oborudovanie, instrumenty) = Metal Working and Material Science*, 2025, vol. 27, no. 3, pp. 122–136. DOI: 10.17212/1994-6309-2025-27.3-122-136. (In Russian).

Introduction

Steels are currently among the most widely used materials in various industrial applications because they are easily accessible, machinable, and weldable [1]. The surfaces of machine parts, tools, and fasteners are exposed to external forces and must possess enhanced strength and wear resistance. Typically, improved mechanical properties of the steel surface can be achieved by modifying the microstructure and chemical composition. This is usually accomplished by using high-carbon and alloy steels as well as various thermal or thermochemical treatments [1, 2].

*** Corresponding author**
Karlina Yulia I., Ph.D. (Engineering), Research Associate
National Research Moscow State Construction University,
Yaroslavskoe shosse, 26,
129337, Moscow, Russian Federation
Tel.: +7 914 879-85-05, **e-mail:** jul.karlina@gmail.com

The effectiveness of heat treatment applied to carbon steels (C% < 0.25) remains limited because such treatment does not sufficiently improve surface properties (hardness, wear and impact resistance, fatigue, etc.) to meet the stringent surface requirements of contacting parts [1–10].

Among chemical-thermal treatment methods, carburization (using solid, gas, or liquid saturating media) is one of the most effective processing techniques. It aims to enrich the surface with carbon in the atomic state (from 0.7 to 0.9 wt.%) by diffusion into the austenite phase (at temperatures from 870 to 980 °C depending on the process), followed by quenching and tempering to enhance the mechanical properties of the surface according to the decreasing carbon gradient at a very limited depth, without affecting the core [1–5]. Taking this into account, it becomes possible to reduce the cost of the final product by using carbon steels (*C*% < 0.25) instead of expensive high-carbon alloy steels. On the other hand, the presence of carbon limits grain refinement on the steel surface, which suppresses the mobility of plastic deformation during solid-to-solid interaction [5–8].

Recently, various researchers have actively developed metal surface layers with gradient solid phases, using different technological methods of surface alloying with carbon, nitrogen, boron, etc. [6, 7].

In [7–13], studies were conducted on the influence of alloying elements such as *Si*, *Ni*, *Cr*, and *Mo* on the carburization characteristics of steels. A significant influence of these alloying elements on the carburization behavior of *AISI 1018*, *4820*, *5120*, and *8620* steels was demonstrated. The authors consider decarburization as the reverse process of carburization and conclude that alloying elements also significantly affect the decarburization of steel. Experimental results showed that *Si* promotes decarburization of ferrite, whereas *Cr* inhibits it in high-carbon steels.

In [15], the influence of certain alloying elements on the decarburization of *TRIP* steel (transformation-induced plasticity) was studied. Experimental results revealed that increasing the content of *Si* and *P* accelerates decarburization. Decarburization is a process wherein carbon atoms diffuse outward from the material and react with furnace gas. Therefore, the effect of alloying elements on steel decarburization primarily affects the diffusion of carbon atoms.

Many authors [1–8] investigated the thermodynamics and activity coefficients of carbon in *FCC* (face-centered cubic) *Fe–Mn–C*, *Fe–Si–C*, *Fe–Ni–C*, and other ternary alloys. Experimental results showed that *Mn* decreases the activity coefficient of carbon in austenite, which in turn reduces the diffusion coefficient of carbon. Conversely, the effect of *Si* on the diffusion coefficient of *C* in austenite is opposite to that of *Mn*. Although experimental methods can reveal the effect of alloying elements on carbon atom diffusion, elucidating the underlying atomic-level mechanisms remains a challenging practical task.

In the practice of many enterprises, an easily implemented, simple, and inexpensive method of carburizing machine parts and mechanisms made of low-carbon steels is the use of a solid carburizer. In industry [1, 2], a two-stage process is traditionally applied: the first stage involves saturating parts with carbon using a solid carburizer followed by air cooling, and the second stage involves hardening and tempering. To reduce carburization period, the heating and equalizing temperature is set in the range of 900–1150 °C [10, 11]. A mandatory requirement for parts subjected to such processing is the allowance of 1–3 mm for subsequent machining in order to remove the decarburized layer. The addition of a large amount of carbon and other alloying elements to these steels leads to serious segregation of composition and surface decarburization of the products.

It has been reported that composition segregation and decarburization have a negative effect on impact toughness, fatigue life, wear resistance, and other properties critical to the performance of medium carbon steels [4–7]. Decarburization reduces surface hardness and fatigue strength of steel, thereby shortening its service life [1, 2, 8–13].

Decarburization of the steel surface results in insufficient hardness in the surface region due to the reduction of carbon content, which greatly reduces fatigue life. Obviously, when steel is heated to high temperatures without a protective atmosphere, the surface layer reacts with oxygen, carbon dioxide, or steam in the furnace atmosphere, causing oxidation and decarburization simultaneously [1, 2]. Decarburization is a classic surface degradation phenomenon in the heat treatment of steels [14].

To prevent decarburization, considerable efforts have been made to develop anti-decarburization coatings [6–10]. Decarburization of steel is influenced by many factors, including heating temperature and heating period [1, 2], atmosphere [12, 13], alloying elements [2, 7, 9], scale layer characteristics [1], electric field [2], etc. Among these, heating temperature and heating period have been proposed as the two most important control variables according to practical experience [1, 2, 15, 16–22].

The purpose of this work is to evaluate the effects of heating temperature during carburizing and quenching, as well as equalizing period, on the depth of the decarburized layer formed during quenching.

Materials and methods

The chemical composition of the steel in the delivered condition was determined using an optical emission spectrometer, model *LAVFA18B Spectrolab*. For this study, non-alloyed hypoeutectoid Steel 20, compliant with *GOST 1050-2013*, with an initial ferrite-pearlite microstructure, was selected. Rectangular samples measuring approximately 50 mm × 10 mm × 10 mm were cut from a rolled sheet of Steel 20. Mechanical cleaning and grinding of the samples were performed; the surfaces were free of oxide traces.

The carburizer used as the cementing mixture consisted of charcoal grains sized 3.6–10 mm, coated with a barium carbonate film according to *GOST 2407–83*. Carbon saturation was carried out on one side (the side in contact with the poured carburizer), while the reverse surface of the samples was protected by a layer of clay. The samples were placed in a metal container and covered with a 25–30 mm layer of carburizer. The container was sealed with a lid. The operating temperature for carbon saturation of the sample surfaces was set at 900 °C, with a saturation period of 4–8 hours [1, 2]. After saturation, the container with samples was removed from the furnace and cooled in air.

Samples were cleaned of scale using a grinding machine. The influence of surface oxides on decarburization kinetics was eliminated by grinding the samples before quenching, as surface oxides increase the apparent decarburization [1, 2]. Quenching was performed in a furnace in air (humidity was not measured) at furnace temperatures of 780 °C, 850 °C, and 950 °C, with equalizing periods of 4 and 6 hours, using a laboratory electric resistance furnace with a chamber volume of $V = 22$ dm³.

Each sample was placed at the same position in the preheated furnace on a refractory brick in the chamber's center. This ensured identical conditions and the fastest possible heating of each sample to the quenching temperature.

Heating temperatures were monitored using a certified contact thermocouple, which was in contact with the side surface of the sample during heating (introduced into the furnace through a small hole in the furnace door). Heating period was counted from the moment the control thermometer inside the furnace reached the target temperature. Temperature fluctuations during heating were within the range of $T_a - 1\ °C \le T \le T_a + 3\ °C$, where T_a is the ambient temperature. After equalizing, quenching was carried out in water. The depth of decarburization [1, 2, 14] was investigated using optical microscopy by two methods: the traditional method using an optical microscope equipped with a grid, and computer-assisted measurement based on the image displayed on the screen. Metallographic samples were prepared by wet grinding with *SiC* paper up to 4,000 grit, polishing with ¼ μm diamond paste, and etching with 3% HNO_3 in ethanol.

Decarburization varies on different surfaces (top and side surfaces exposed to atmosphere, and the bottom surface in contact with the refractory brick, including edges and corners) due to differences in oxidation states. Typically, decarburization is more pronounced on surfaces with lower oxidation capacity; therefore, the bottom surfaces usually exhibit stronger decarburization [13, 15].

This study focused exclusively on flat surfaces exposed to the atmosphere. Decarburization was measured on three sections perpendicular to the long side of the sample on the top and both side surfaces.

Results of the research

Carbon content analysis

The surface layer of the low-alloy steel initially had a relatively low carbon content of approximately $\alpha = (0.21 \pm 0.06)$ wt. %. before carburization, which corresponded to the initial carbon amount of low alloy steels, as shown in Table.

Effect of carburization period on carbon content in Steel 20

	Chemical elements, %						
	C	***Si***	***Mn***	***S***	***P***	***Ni***	***Cr***
GOST 1050-2013	0.17–0.24	0.17–0.37	0.35–0.65	up to 0.035	up to 0.030	up to 0.30	up to 0.25
Fact	0.21	0.27	0.36	up to 0.035	up to 0.030	up to 0.30	up to 0.25
Cementation period: 4 hours	0.53	0.27	0.36	up to 0.035	up to 0.030	up to 0.30	up to 0.25
Cementation period: 6 hours	0.68	0.27	0.36	up to 0.035	up to 0.030	up to 0.30	up to 0.25

However, after carburization of varying duration, the carbon content in the surface layer gradually increased. Specifically, after 4 hours of carburization, the carbon content reached $\alpha = (0.53 \pm 0.016)$ wt. %, after 6 hours, it reached $\alpha = (0.68 \pm 0.012)$ wt. %. Experiments with longer saturation duration were also carried out.

The results of the experiments are shown in Fig. 1–3. It was found that increasing the saturation period of the samples with carbon to 8 hours increases the carbon content in the surface layer of steel. Moreover, with saturation of 8 hours or more, the samples completely have a pearlite structure with a carbon content of 0.8 %. Based on these experiments, it was subsequently decided to reduce the saturation time to 2 hours in order to minimize the experiments.

Microstructural analysis

After carburizing, a significant increase in the surface layer thickness by more than 41 % was observed as the equalizing period increased (Figs. 1 and 2). The thickness increased from approximately 1,100 μm to more than 1,500 μm, as shown in Fig. 3.

As the equalizing period in the furnace increases, a decarburized layer appears during heating for hardening. This can be seen from the results of microhardness measurements in Fig. 4 and the metallographic analysis of the surface in Fig. 5. The effect of heating temperature on hardening is shown in Fig. 6.

In our experiments, it was found that temperature played an important role in decarburization. At 700 °C, no decarburization phenomenon was observed, indicating that the decarburization reaction did not occur in the samples below 700 °C. When the temperature exceeds 750 °C, the sample exhibits obvious

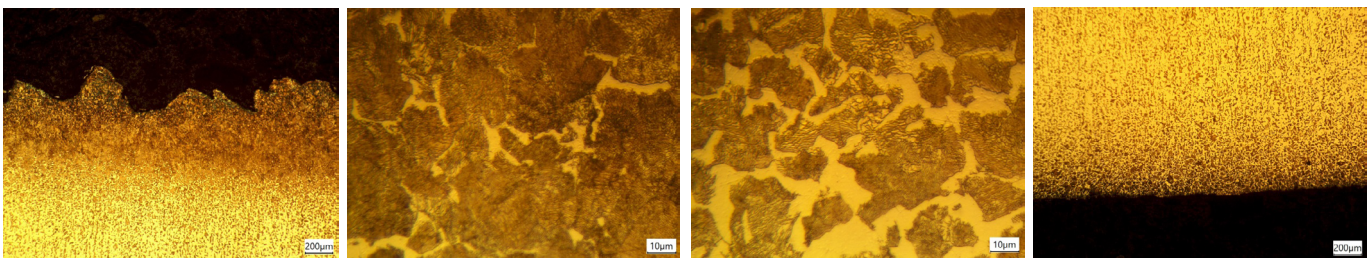

a *b* *c* *d*

Fig. 1. The microstructure of the cemented layer of Steel 20 after equalizing for 4 hours at 900 °C:
a – surface layer; *b* – at a depth of 100 μm; *c* – transition layer to the base metal; *d* – reverse side of the sample

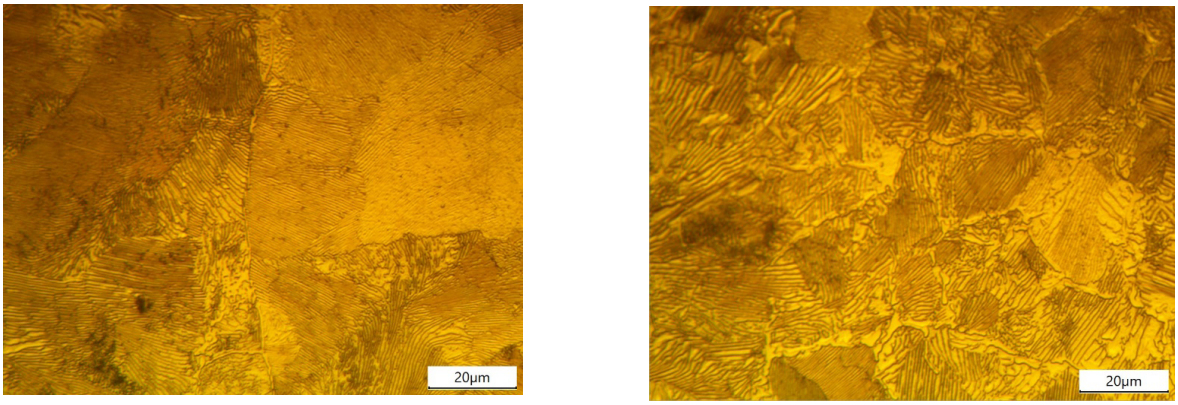

a *b*

Fig. 2. Pearlite structure in the carburized layer of Steel 20 after equalizing for 6 hours at 900 °C:
a – pearlite structure in the surface layer; *b* – in the middle of the sample

Fig. 3. Comparative evaluation of carbon content, microhardness, and depth of the cemented layer as a function of saturation period

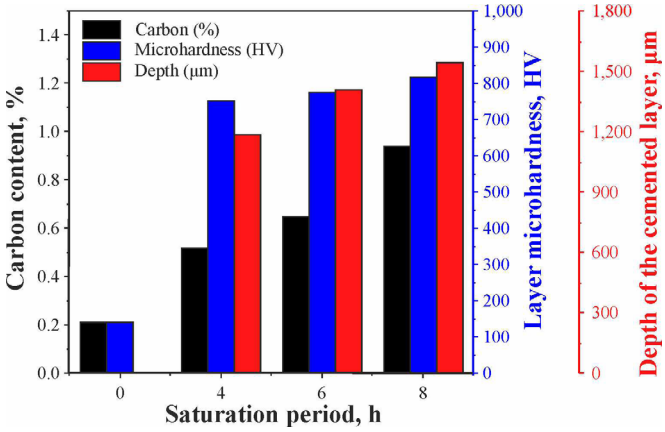

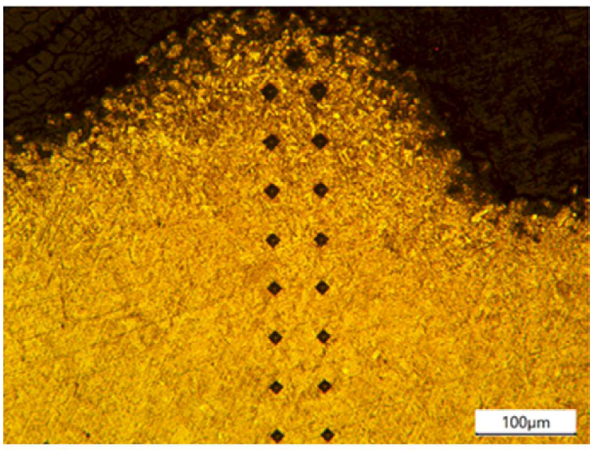

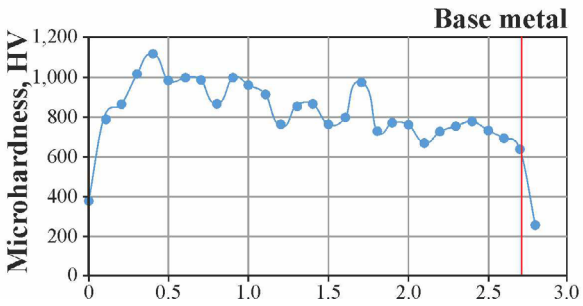

Fig. 4. Photo of point of indentation and graph of microhardness distribution across the depth of the surface cemented layer

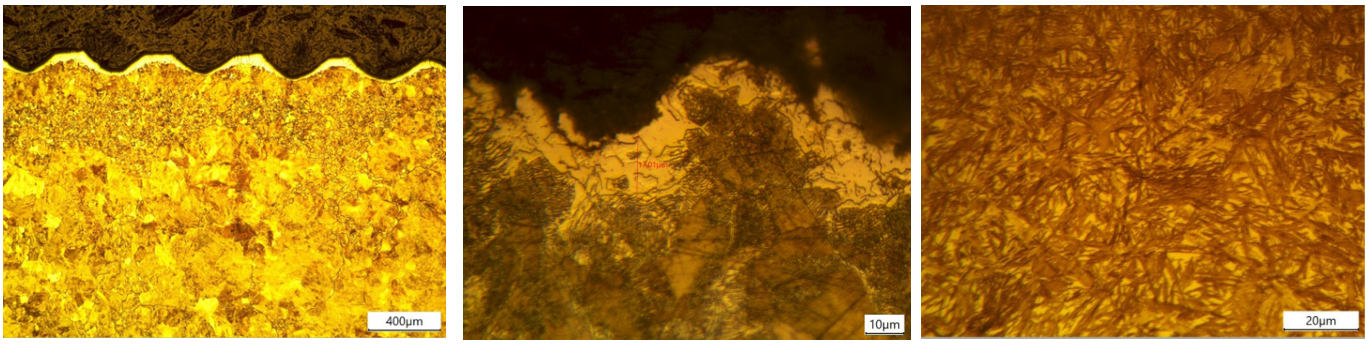

a *b* *c*

Fig. 5. Photo of the surface layer after heating for hardening at 950 °C and equalizing for 6 hours:
a and *b* – decarburized layer at different magnifications; *c* – quenched martensite in the surface layer

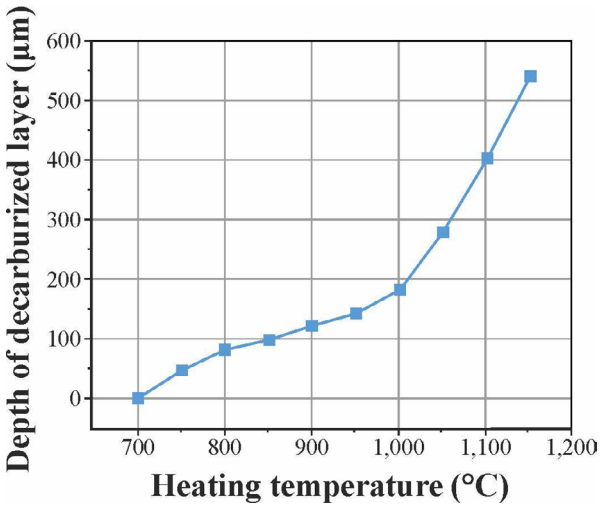

Fig. 6. Depth of decarburization as a function of heating temperature (equalizing for 50 min)

decarburization, and the ferrite structure becomes columnar, perpendicular to the decarburization surface. A partly decarburized layer appears in the sample at 850 °C, and the thickness of the fully decarburized layer decrease. The decarburized layer is composed of both complete and partial decarburization zones. Above 900 °C, the sample mainly shows a partly decarburized layer, because at this temperature the steel structure is completely austenitic, as ferrite and pearlite (a mixture of cementite and ferrite) are transformed into austenite. Carbon from austenite passes into the furnace atmosphere and interacts with furnace oxygen. As a result, the steel becomes depleted in carbon content. The average depth of the fully decarburized layer of each sample is shown in Fig. 7. As shown in Fig. 6, at a heating temperature below 1,000 °C, the thickness of the total decarburized layer increases slowly. However, above 1,000 °C, the thickness increases rapidly, showing exponential growth. The experiments showed the effect of heating and equalizing periods on the depth of the decarburized layer (Fig. 7).

The depth of the decarburized layer was measured using an optical microscope, and the average decarburization depth of the samples is shown in Fig. 6. As can be seen in Fig. 6, the depth of the decarburized layer of the samples increased exponentially with the heating temperature, and parabolically with the equalizing period in the furnace at different temperatures (Fig. 7), with the growth rate gradually slowing down.

To protect the surface of the cemented layer, it is necessary to apply a coating that will protect the surface from contact with the furnace atmosphere during heating for hardening (Fig. 8). It is known that the effective depth of the cemented layer is related to the hardness in depth after hardening, which ranges from 555 to 600 HV (Fig. 8).

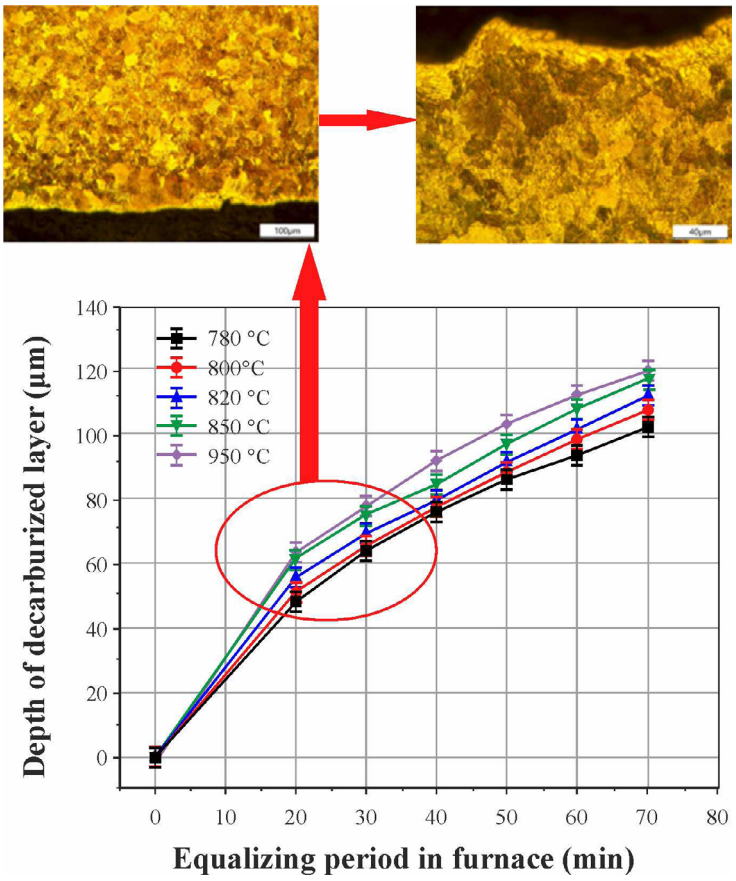

Fig. 7. The effect of heating temperature and equalizing period on the overall depth of decarburization

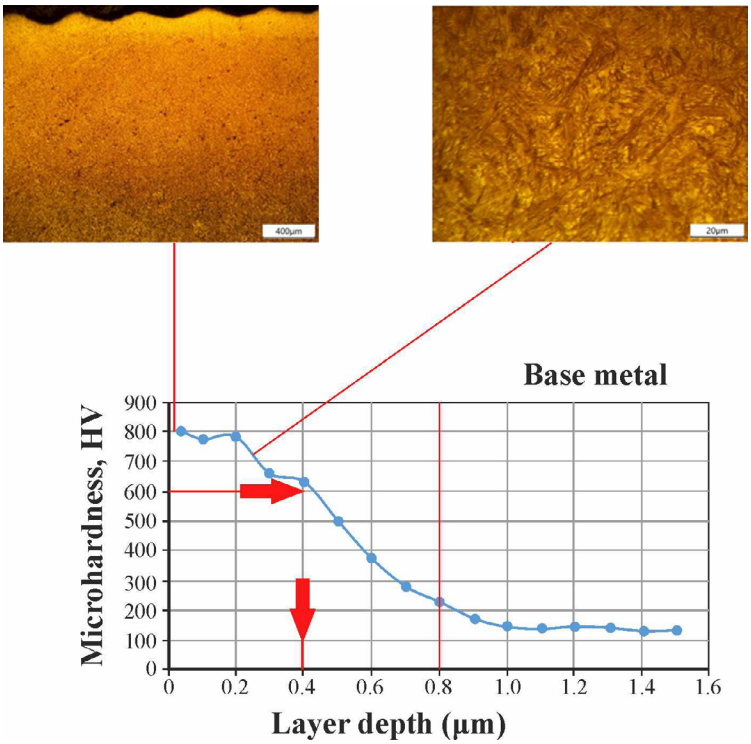

Fig. 8. Microstructure of the surface layer after cementation quenching with surface protection from oxygen

Discussion of the results

From the analysis of the literature, it is evident [1–12, 17–21] that the theoretical discussion of the depth of decarburization during heating remains a debatable issue.

The works [1, 2] provide information that in 1946 *Pennington* conducted a comprehensive study of the decarburization of carbon steel in the temperature range of 691–927 °C in an atmosphere containing 20 % $H_2O - H_2$, in which oxidation of steel could not occur. In this study, it was found that a ferrite "band" formed on the steel surface at 732–893 °C, but not at 691 °C and 927 °C, while the maximum ferrite thickness was observed at 790–815 °C. *Pennington* explained the decrease in ferrite thickness above 905 °C by a decrease in the solubility of carbon in ferrite to zero at 905 °C. One of the limitations of *Pennington's* analysis was the assumption that the carbon concentration in the formed ferrite was constant throughout the ferrite layer and, therefore, that carbon diffusion within the ferrite did not contribute to its growth. Simultaneous oxidation and decarburization were studied by *Birks* and colleagues in 1970. Based on these studies, it was stated that "the mechanism by which decarburization of steels occurs has been well studied, particularly in the case of plain carbon and low alloy steels" [1, 2]. However, the scope of the studies by *Birks* et al. was limited. First, the studies focused on decarburization occurring only in the austenite. Second, although it was recognized that in an oxidizing atmosphere decarburization occurs through a reaction between the scale and dissolved carbon in the steel, *Birks* and colleagues continued to assume that the carbon concentration at the scale-steel interface was zero because of its low value.

It is known that decarburization and surface oxidation occur simultaneously on the steel surface when heated in an oxidizing environment. In essence, decarburization is a reaction between carbon in the matrix and oxygen, while oxidation is a reaction between iron and oxygen. Therefore, decarburization is closely related to oxidation, and the relationship between them is competitive. The formation of an oxide layer on the steel surface consumes part of the decarburized surface layer and, thus, reduces the final observed decarburization thickness. Therefore, to obtain more accurate results, it is necessary to take into account the oxidation process. The absolute thickness of the total decarburized layer can be considered as the sum of the thicknesses of the observed total decarburization and the oxide scale. In practice, the thickness of the oxide scale cannot be measured accurately, since the oxide layer tends to flake off from the sample surface during the cooling period and subsequent manipulations.

When examining the *Fe–O* phase diagram [1, 2], we assumed that the oxide layer on the surface of iron and unalloyed steel consists of only one oxide, *FeO*, which is formed during heating in air at temperatures ($\boldsymbol{T}$ > 570 °C). In reality, according to [1, 2], the high partial pressure of oxygen and different iron chemical valence create an oxide layer consisting of three different oxides at these temperatures. The sequence from the oxide with the least amount of oxygen, closest to the metal, to the oxide with the highest amount of oxygen, closest to the atmosphere, has been recorded as: *FeO* / Fe_3O_4 / Fe_2O_3 — wustite / magnetite / hematite [1, 2]. The layer thickness is generally constant at ($\boldsymbol{T}$ > 700 °C), and its composition is approximately 95 % *FeO*, 4 % Fe_3O_4, and 1 % Fe_2O_3 [1, 2].

At temperatures ($\boldsymbol{T}$ = 570–800 °C), however, results can be found [16–22] that deviate both in terms of composition and thickness of the individual layers, demonstrating the complexity of the oxidation of iron and unalloyed steel in this temperature range [14]. The formation of a three-layer oxide layer can be explained simply using direct oxidation chemical reactions. The mechanism of formation of a three-layer oxide layer at the *FeO*/Fe_3O_4 and Fe_3O_4/Fe_2O_3 phase boundaries remains a subject of discussion due to its complexity, which is a consequence of specific transport processes through individual oxide layers [2, 15, 16].

When discussing carbon oxidation, it is necessary to take into account the microstructure of the steel at the heating temperature and the temperature range of stability for CO_2 and *CO*. Carbon in unalloyed hypoeutectoid steel at temperatures $\boldsymbol{T} > A_{C1}$ is present only in solid solution dissolved in *Fe*-α (ferrite) and *Fe*-γ (austenite). Ferrite is stable at $\boldsymbol{T} < A_{C3}$, and austenite is stable at $\boldsymbol{T} > A_{C1}$. Carbon reacts with oxygen to form *CO* and CO_2 during heating of steel in air. The reactions of direct oxidation of carbon by oxygen ($C + O_2 \rightarrow CO_2$ and $2C + O_2 \rightarrow 2CO$) intersect at approximately T ≈ 700 °C [1, 2]. The lines of both reactions show that at $\boldsymbol{T}$ > 700 °C, *CO* is more stable, or that *CO* is preferentially formed at $T > A_{C1}$ [1, 2].

This means that, relative to the *Boudouard* equilibrium ($C + CO_2 \leftrightarrow 2CO$), the reaction proceeds from left to right at T > 700 °C) [1, 2, 12, 17], indicating a tendency towards decarburization at $\boldsymbol{T} > A_{C1}$. Since an increase in temperature favors the preferential oxidation of carbon to form *CO*, the equilibrium concentration of *CO* in the resulting gas mixture also increases [1, 2].

According to [20–22], it is important to know that gas mixtures ($CO + CO_2$) cause decarburization of steel if their composition lies below or to the right of the equilibrium line for this steel, while they cause carburization if their composition lies above or to the left of this line.

During heating for quenching in air, decarburization of steel is initiated by the general oxidation of the steel surface due to the high partial pressure of oxygen. The oxidation and decarburization reactions occur simultaneously; therefore, various effects on both processes are intertwined, some directly proportional and some inversely proportional. As mentioned earlier, decarburization is visible only if the oxidation of the steel surface is slower than its decarburization, i.e., when the oxidation of carbon and the rate of carbon diffusion are greater than the oxidation rate. Visible decarburization depends on the oxidation potential of the atmosphere in the quenching furnace, which also determines the degree of surface oxidation. This is the reason for the large differences in visible decarburization that occur when heating in air or, for example, in a mixture of N_2 + 2% O_2 [8].

Visible decarburization is always greater when heated in low-oxygen atmospheres [8, 10]. It is also influenced by the adherence of the oxide layer to the steel surface (poor adherence of the oxide layer increases decarburization due to a decrease in the oxidation rate) and its permeability to gases (an impermeable oxide layer reduces decarburization), the carbon content of the steel, and the cooling rate after heating, while different alloying elements affect the kinetics of oxidation and decarburization. At low cooling rates, decarburization also occurs during cooling, especially in the two-phase (α + γ) region where the surface ferrite layer thickens due to slower oxidation. In hypoeutectoid unalloyed steels, the overall visible decarburization decreases with higher cooling rates. This is a consequence of the decrease and convergence of the temperatures A_{r3} and A_{r1} and the resulting decrease in ferrite content due to the increased pearlite content [1, 2]. At some point for each steel characteristic, the critical cooling rate is reached, A_{r3} and A_{r1} temperatures become equal. At this point, there is no longer any hypoeutectoid ferrite in the microstructure. If the cooling rate is thus high enough for the partially decarburized layer, then hypoeutectoid ferrite will no longer form in this layer either, and only pearlite will exist there.

At even higher cooling rates, bainite or martensite is formed in the partially decarburized layer. Because of this, the partially decarburized layer is not fully visible at higher cooling rates and may disappear completely at a sufficiently high cooling rate, leaving only the fully decarburized surface layer visible. The metallographically determined decarburization depth is always smaller than the actual depth [1, 2]. In metallographic analysis, it is also necessary to take into account the limited ability of the human eye to detect small differences in the content of ferrite and pearlite or globular cementite in ferrite (spheroidized state), which further reduces the estimated thickness of the decarburized layer and increases the observation error. More accurate values for the decarburization depth are determined by microhardness measurements, but these are still not as accurate as the actual depths measured by chemical analysis [19, 22].

Thus, our experiments show a significant increase in carbon content by more than three times with longer equalizing periods during the carburizing process (Fig. 3).

The observed increase in carbon content can be explained by carbon diffusion, which is influenced by both the absorption rate and the carburizing duration. This diffusion process facilitates the reaction with iron in the low alloy gear steel, resulting in the formation of a new carbon-based phase. A similar trend of increasing carbon content in the surface layer of *Fe-C-Mn* steels with longer carburizing periods has been observed [14–20]. The increase in thickness indicates successful diffusion of carbon into the surface layer during carburizing. As carbon diffuses into the steel, it combines with iron to form a new carbon-based phase, resulting in an increase in the layer thickness. This increased thickness is desirable, as it implies improved mechanical properties after quenching.

Conclusion

1. Oxidation, maximum visible surface decarburization, and the completely decarburized ferrite layer increase with increasing heating period during quenching in a furnace with an air atmosphere, following the parabolic growth law. It is shown that with increasing heating temperature for quenching, the depth of the decarburized layer increases exponentially. The decarburization temperature plays a more important role in the decarburization rate compared to other influencing factors, since decarburization is a thermally activated process and exhibits high temperature sensitivity.

2. It was found that heating to a quenching temperature of $\boldsymbol{T}$ = 850–870 °C for $\boldsymbol{t}$ = 1 hour, under oxidizing furnace conditions, leads to decarburization of the surface layer to a depth of 5–10 μm.

3. It was found that heating to a quenching temperature of T = 1,100 °C in the oxidizing atmosphere of the furnace, with holding times ranging from 0.5 hours to 2 hours at an ambient temperature of T_a, results in the formation of a ferrite layer with a thickness of 50-100 μm.

References

1. Lakhtin Yu.M. *Metallovedenie i termicheskaya obrabotka metallov* [Metallology and heat treatment of metals]. Moscow, Metallurgiya Publ., 1983. 359 p.

2. Lakhtin Yu.M., Arzamasov B.N. *Khimiko-termicheskaya obrabotka metallov* [Chemical and thermal treatment of metals]. Moscow, Metallurgiya Publ., 1985. 256 p.

3. Choi S., Zwaag S.V.D. Prediction of decarburized ferrite depth of hypoeutectoid steel with simultaneous oxidation. *ISIJ International*, 2012, vol. 52 (4), pp. 549–558. DOI: 10.2355/isijinternational.52.549.

4. Zhang C.L., Xie L.Y., Liu G.L., Chen L., Liu Y.Z., Li J. Surface decarburization behavior and its adverse effects of air-cooled forging steel C70S6 for fracture splitting connecting rod. *Metals and Materials International*, 2016, vol. 22 (5), pp. 836–841. DOI: 10.1007/s12540-016-5657-x.

5. Carroll R.I., Beynon J.H. Decarburisation and rolling contact fatigue of a rail steel. *Wear*, 2006, vol. 260 (4–5), pp. 523–537. DOI: 10.1016/j.wear.2005.03.005.

6. Ren C.X., Wang D.Q.Q., Wang Q., Guo Y.S., Zhang Z.J., Shao C.W., Yang H.J., Zhang Z.F. Enhanced bending fatigue resistance of a 50CrMnMoVNb spring steel with decarburized layer by surface spinning strengthening. *International Journal of Fatigue*, 2019, vol. 124, pp. 277–287. DOI: 10.1016/j.ijfatigue.2019.03.014.

7. Zhao X.J., Guo J., Wang H.Y., Wen Z.F., Liu Q.Y., Zhao G.T., Wang W.J. Effects of decarburization on the wear resistance and damage mechanisms of rail steels subject to contact fatigue. *Wear*, 2016, vol. 364–365, pp. 130–143. DOI: 10.1016/j.wear.2016.07.013.

8. Li S., Feng H., Wang S., Gao J., Zhao H., Wu H., Xu S., Feng Q., Li H., Liu X., Wu G. Phase transformation behaviors of medium carbon steels produced by twin roll casting and compact strip production processes. *Materials*, 2023, vol. 16 (5), p. 1980. DOI: 10.3390/ma16051980.

9. Xiao Z., Huang Y., Liu H., Wang S. Hot tensile and fracture behavior of 35CrMo steel at elevated temperature and strain rate. *Metals*, 2016, vol. 6 (9), p. 210. DOI: 10.3390/met6090210.

10. Wang X., Lianqi W., Zhou X., Zhang X., Shufeng Y., Chen Y. Protective bauxite-based coatings and their anti-decarburization performance in spring steel at high temperatures. *Journal of Materials Engineering and Performance*, 2013, vol. 22, pp. 753–758. DOI: 10.1007/s11665-012-0309-x.

11. Chen Y.R., Zhang F., Liu Y. Decarburization of 60Si2MnA in 20 Pct H_2O-N_2 at 700 °C to 900 °C. *Metallurgical and Materials Transactions A*, 2020, vol. 51, pp. 1808–1821.

12. Chen Y.R., Zhang F. New development in decarburization research and its application to spring steels. *High Temperature Corrosion of Mater*, 2023, vol. 100, pp. 109–143. DOI: 10.1007/s11085-023-10181-3.

13. Gildersleeve M.J. Relationship between decarburisation and fatigue strength of through hardened and carburising steels. *Materials Science and Technology*, 1991, vol. 7 (4), pp. 307–310.

14. GOST R 54566–2011. *Standartnye metody ispytanii dlya otsenki glubiny obezuglerozhennogo sloya* [State Standard R 54566–2011. Steel. Standard test methods for estimating the depth of decarburized layer]. Moscow, Standartinform Publ., 2014. 15 p.

15. Zorc M., Nagode A., Burja J., Kosec B., Zorc B. Surface decarburization of the hypo-eutectoid carbon steel C45 during annealing in steady air at temperatures $T > A_{C1}$. *Metals*, 2018, vol. 8, p. 425. DOI: 10.3390/met8060425.

16. Stepankin I.N., Pozdnyakov E.P. K voprosu izgotovleniya melkorazmernogo shtampovogo instrumenta iz ekonomno legirovannykh stalei s diffuzionnym uprochneniem poverkhnostnogo sloya [To the issue of manufacturing of small-size stamping tools from economically alloyed steels with diffusion hardening of the surface layer].

Kuznechno-shtampovochnoe proizvodstvo. Obrabotka materialov davleniem = Forging and Stamping Production. Material Working by Pressure, 2015, no. 9, pp. 25–32.

17. Çalik A. Effect of cooling rate on hardness and microstructure of AISI 1020, AISI 1040 and AISI 1060 Steels. *International Journal of Physical Sciences*, 2009, vol. 4 (9), pp. 514–518.

18. Ramesh B., Vempati S.R., Manjunath C., Elsheikh A.H. Examination of minimum quantity lubrication performance in the hard turning of AISI/SAE 1060 high-carbon steel. *Journal of Materials Engineering and Performance*, 2024, vol. 34 (13), pp. 136861–13696. DOI: 10.1007/s11665-024-10070-z.

19. Dewangan S., Mainwal N., Khandelwal M., Jadhav P.S. Performance analysis of heat treated AISI 1020 steel samples on the basis of various destructive mechanical testing and microstructural behavior. *Australian Journal of Mechanical Engineering*, 2022, vol. 20 (1), pp. 74–87. DOI: 10.1080/14484846.2019.1664212.

20. Chen R.Y., Yeun W.Y.D. Review of the high-temperature oxidation of iron and carbon steels in air or oxygen. *Oxidation of Metals*, 2003, vol. 59 (5), pp. 433–468.

21. Voort G.F.V. Understanding and measuring decarburization. *AM&P Technical Articles*, 2015, vol. 173 (2), pp. 22–27.

22. Konstantinova M.V., Balanovskiy A.E., Gozbenko V.E., Kargapoltsev S.K., Karlina A.I., Shtayger M.G., Guseva E.A., Kuznetsov B.O. Application of plasma surface quenching to reduce rail side wear. *IOP Conference Series: Materials Science and Engineering*, 2019, vol. 560 (1), p. 012146. DOI: 10.1088/1757-899X/560/1/012146.

23. Yelemessov K., Baskanbayeva D., Martyushev N.V., Skeeba V.Y., Gozbenko V.E., Karlina A.I. Change in the properties of rail steels during operation and reutilization of rails. *Metals*, 2023, vol. 13, p. 1043. DOI: 10.3390/met13061043.

24. Shtayger M.G., Balanovskiy A.E., Kargapoltsev S.K., Gozbenko V.E., Karlina A.I., Karlina Yu.I., Govorkov A.S., Kuznetsov B.O. Investigation of macro and micro structures of compounds of high-strength rails implemented by contact butt welding using burning-off. *IOP Conference Series: Materials Science and Engineering*, 2019, vol. 560 (1), p. 012190. DOI: 10.1088/1757-899X/560/1/012190.

25. Balanovskiy A.E., Shtayger M.G., Karlina A.I., Kargapoltsev S.K., Gozbenko V.E., Karlina Yu.I., Govorkov A.S., Kuznetsov B.O. Surface hardening of structural steel by cathode spot of welding arc. *IOP Conference Series: Materials Science and Engineering*, 2019, vol. 560 (1), p. 012138. DOI: 10.1088/1757-899X/560/1/012138.

26. Skeeba V.Yu., Ivancivsky V.V., Kutyshkin A.V., Parts K.A. Hybrid processing: the impact of mechanical and surface thermal treatment integration onto the machine parts quality. *IOP Conference Series: Materials Science and Engineering*, 2016, vol. 126 (1), p. 012016. DOI: 10.1088/1757-899x/126/1/012016.

27. Efremenkov E.A., Martyushev N.V., Skeeba V.Yu., Grechneva M.V., Olisov A.V., Ens A.D. Research on the possibility of lowering the manufacturing accuracy of cycloid transmission wheels with intermediate rolling elements and a free cage. *Applied Sciences*, 2022, vol. 12 (1), p. 5. DOI: 10.3390/app12010005.

28. Martyushev N.V., Skeeba V.Yu. The method of quantitative automatic metallographic analysis. *Journal of Physics: Conference Series*, 2017, vol. 803 (1), p. 012094. DOI: 10.1088/1742-6596/803/1/012094.

29. Skeeba V.Yu., Ivancivsky V.V. Reliability of quality forecast for hybrid metal-working machinery. *IOP Conference Series: Earth and Environmental Science*, 2018, vol. 194 (2), p. 022037. DOI: 10.1088/1755-1315/194/2/022037.

30. Zverev E.A., Skeeba V.Y., Skeeba P.Y., Khlebova I.V. Defining efficient modes range for plasma spraying coatings. *IOP Conference Series: Earth and Environmental Science*, 2017, vol. 87 (8), p. 082061. DOI: 10.1088/1755-1315/87/8/082061.

31. Skeeba V.Yu. Hybrid process equipment: improving the efficiency of the integrated metalworking machines initial designing. *Obrabotka metallov (tekhnologiya, oborudovanie, instrumenty) = Metal Working and Material Science*, 2019, vol. 21, no. 2, pp. 62–83. DOI: 10.17212/1994-6309-2019-21.2-62-83. (In Russian).

32. Borisov M.A., Lobanov D.V., Yanyushkin A.S., Skeeba V.Yu. Investigation of the process of automatic control of current polarity reversal in the conditions of hybrid technology of electrochemical processing of corrosion-resistant steels. *Obrabotka metallov (tekhnologiya, oborudovanie, instrumenty) = Metal Working and Material Science*, 2020, vol. 22, no. 1, pp. 6–15. DOI: 10.17212/1994-6309- 2020-22.1-6-15. (In Russian).

33. Mamadaliev R.A., Bakhmatov P.V., Martyushev N.V., Skeeba V.Y., Karlina A.I. Influence of welding regimes on structure and properties of steel 12KH18N10T weld metal in different spatial positions. *Metallurgist*, 2022, vol. 65 (11–12), pp. 1255–1264. DOI: 10.1007/s11015-022-01271-9.

34. Balanovsky A.E., Shtayger M.G., Kondrat'ev V.V., Van Huy V., Karlina A.I. Plasma-arc surface modification of metals in a liquid medium. *IOP Conference Series: Materials Science and Engineering*, 2018, vol. 411 (1), p. 012013. DOI: 10.1088/1757-899X/411/1/012013.

35. Karlina A.I., Karlina Y.I., Gladkikh V.A. Studying the microstructure, phase composition, and wear resistance of alloyed layers after laser surface melting of low-carbon steel 20. *Metallurgist*, 2024, vol. 68 (5), pp. 757–766. DOI: 10.1007/s11015-024-01782-7.

36. Karlina A.I., Karlina Y.I., Kondratiev V.V., Kononenko R.V., Breki A.D. Study of wear of an alloyed layer with chromium carbide particles after plasma melting. *Crystals*, 2023, vol. 13 (12), p. 1696. DOI: 10.3390/cryst13121696.

Conflicts of Interest

The authors declare no conflict of interest.